Comparative study of variational and level set approaches for shape extraction in cardiac CT images

Leiner Barba-J[a], Boris Escalante-Ramírez[a], Enrique Vallejo[b]

[a] Advanced Laboratory of Image Processing – Signal Processing Dep.–Engineering Faculty
[b] PET/CT Cyclotron Unity – Research Building
Universidad Nacional Autónoma de México, México D.F.

ABSTRACT

Variational approaches based on level set representation have become some of the most important methodologies used to handle the segmentation tasks of biological structures in medical images. Because segmentation is one of the most challenging processes in medical applications, all the methods fail to achieve perfect results. The major problems are due to noise, poor contrast and high variation of structure shapes. In this paper, we review the principal level set – based methods that have been designed for image segmentation applications. These approaches include: Geodesic Active Contour, Chan-Vese Functional and Geodesic Active Regions. We also shortly analyze one of the first methods proposed for shape extraction in images by using level set representation (Malladi's method[6]). We make a comparative study of the performance obtained for each method applied on cardiac CT images which present strong and very marked differences regarding the contrast and shape variation of the structures. Left ventricle is selected as our structure of analysis. Sensitivity, specificity and a distance metric to compare similarities between shapes are used to evaluate the performance of the methods.

Keywords: Level set methods, image segmentation, cardiac CT images

1. INTRODUCTION

Image segmentation is one of the previous tasks before applying other high level procedures in medical image applications. Obtaining good segmentations is so important that most advanced processes do not work efficiently when objects from images are erroneously extracted. Functional and anatomical analysis of each part of the human body[1], volumetric measurements and guided surgery procedures[2] are some examples in which the segmentation performance is highly required. Hundreds of works have been developed during the last 20 years, but most of them fail to work correctly in the whole range of images for which they were created. In the area of medical image analysis, active contour based on implicit[3-6] and explicit representation[7], active shape and appearance models[8,9] are the most famous methodologies for segmentation. In this work, we pay special attention to the variational methods based on level sets.

Since its discovering by Osher and Shetian[10], level set has been extensively employed in medical images for a great amount of segmentation applications[11-13]. The main reason of its usefulness is the ability to break and merge when changes of topology are presented. The implicit representation of moving contours using level sets makes easier the shape extraction procedure. Issues related to computer implementations, discretization and facility to extend the methods to higher dimensions are also strong arguments to choose level set approaches.

On the other hand, cardiac images has been the objective of analysis for an uncountable number of researchers during the last decades. For this subject, level set approaches have found one of the main applications and have been intensively used in this types of images. The uses include ultrasound[14], MR (Magnetic Resonance)[15], PET (Positron Emission Tomography)[16] and CT (Computed Tomography)[17] modalities, in which chambers segmentation (specially the left ventricle) cover most of the articles.

In this work, we want to review the basic principles of the level set methodology for the segmentation of cardiac CT images. This type of medical data represents one of the main used modalities for heart evaluation. Calculating the left ventricle dimensions or its size in each phase of the cardiac cycle constitutes an important task to assess the heart mechanical function. The ejection fraction is a measure that can be obtained with the segmentation. Even though many

IX International Seminar on Medical Information Processing and Analysis, edited by
Jorge Brieva, Boris Escalante-Ramírez, Proc. of SPIE Vol. 8922, 89220Y · © 2013
SPIE · CCC code: 0277-786X/13/$18 · doi: 10.1117/12.2035502

researchers have been working on new segmentation algorithms applied to cardiac images, the great variability found in the heart has made that the segmentation task still remain as an open issue. For contrast cardiac CT, it is even more difficult to have a universal segmentation method. In our analysis, we include the principal techniques based on level sets that were developed. As mentioned, tens of segmentation methods based on the level set theory have been created during the lasts 25 years, making extremely difficult the analysis of all of them. We selected the most acceptable and famous approaches based on the number of citation received. The selection was made according to the statistical information found in the academic platform Google Scholar. The most cited documents are the Chan-Vese approach[4], Geodesic Active Contour proposed by Caselles et al.[3], Geodesic Active Regions designed by Nikos Paragios[5] and the Malladi et al. method[6], which was the one of the first proposal for extracting shapes by using level sets. Moreover, almost all of the works we found in literature, where level sets are used for medical image segmentation, are modification or combinations of the referenced techniques. Special attention is deserves to those works where significant adaptations are proposed to handle the main problems of the level sets approaches such as re-initialization[18] and conservation of the sign distance function[19]. We prove each of the analyzed method in cardiac CT images. For this purpose, we try to segment the left ventricles in slices taken from axial tomographic studies. We present some characteristics about the algorithmic implementation taken into account for the level set algorithms.

The rest of the paper is organized as follows. In section 2, we describe the four methods and the level set general theory. In section 3 we give some details about the implementation of the algorithms. We also talk about the materials and data. Finally, we present some preliminary results of our analysis and the conclusions in sections 4 and 5 respectively.

2. METHODS

In this section, we describe the principal methods covered by this study. Level sets theory, Geodesic Active Contours[3] Chan-Vese functional[4], and Geodesic Active Regions[5] are briefly depicted here. We remark the principal advantages and problems for each of the methods in segmentation tasks. Strong details about the methods are out of this paper and we recommend the readers to go directly to the referenced works.

2.1 Level Set

Osher and Sethian[10] demonstrated that propagating fronts (fronts evolving in time) can be recovered implicitly as the zero level set of a function with higher dimension. Their demonstration has been extensively used in several fields, acquiring great importance in computer vision for image segmentation. In this last application, it is considered a simple closed curve in the image domain that moves with a specific velocity. The curve is the function that fragments the image in the desired regions.

Let C be a simple and close interface (curve) which is defined in the image domain Ω: $C = (x(s), y(s))$. In segmentation applications, it is considered that the curve is moving or evolving in the normal direction $\boldsymbol{n}$ with a velocity field V:

$$\frac{\partial C}{\partial t} = V\boldsymbol{n} \quad (1)$$

which implies that this active curve is characterized by a one-parameter (time) family of curves. Therefore, it becomes a function that depends on (s,t), i.e, $C: (s,t) \epsilon [0,1] \times R^+ \to C(s,t) = (x(s), y(s), t) \epsilon\, \Omega \times \mathrm{R}^+$. It has been extensively demonstrated that working with the explicit representation of the curve is less convenient for the algorithmic implementation[13, 20]. Problems related to changes of topology, emerging shapes, concavities and others are poorly handled in this case. The nice work made by Stanley Osher et al.[10] allowed that these problems can be easily solved by using an implicit representation of the interface. Therefore, the active curve C can be represented as the zero level set of a function $\varphi: R^2 \times R^+ \to R$. With the implicit representation $\varphi\big(C(s,t)\big) = \varphi(x(s), y(s), t) = 0$, the motion equation (1) is equivalent to:

$$\frac{\partial \varphi}{\partial t} = V\|\nabla\varphi\| \quad (2)$$

where $\|\nabla\varphi\|$ is the gradient magnitude of the level set function, which is defined as: $\forall s, t,\ \ \varphi(s,t) = +d$ out the curve, $\varphi(s,t) - d$ inside the curve, and $\varphi(s,t) = 0$ on the curve, being d a distance function with the property: $\|\nabla\varphi\| = 1$.

For image segmentation applications, the velocity field can depend either on the interface parameters such as the curvature or on the image characteristics (gray level, color, texture, gradient and others). The methods considered in this work are applied to segment the entire image domain in two regions: one or several objects with similar features regarding a common background. Malladi et al.[6] introduced the first approach for extracting objects from an image by employing level sets. Taking advantage of the moving interface, they used the velocity field for the segmentation process. The velocity is then made to be dependant of the object boundaries. When the active curve is at the edges of the objects, the velocity field vanishes. The evolution equation is described as:

$$\frac{\partial \varphi}{\partial t} = V(F + ck)\|\nabla\varphi\| \tag{3}$$

where $(F + ck)$ represents a term of velocity that depends on the curvature k of the level set function; F and c are constant. The velocity V is a function that decreases monotonically whit the image gradient. Two type of functions with this property were proposed: 1) $V(x, y) = \frac{1}{1+|\nabla(G*I(x,y))|^n}$ and 2) $V(x, y) = e^{-|\nabla(G*I(x,y))|}$ where G is a smoothing filter applied on the image I and $n = 1, 2$. The idea behind this method is to stop the evolution of the level set function when the contour (represented as the zero level set) is at the boundaries of the objects. It happens when the gradient obtained from the images is relatively high. Although this method has been proved to have poor performance for real images, we also evaluated it here for our set of cardiac CT images. Below, we outline three of the most popular level set approaches for image segmentation that we used in our analysis.

2.2 Geometric Active Contours - GAC

Caselles et al.[3] and Kichenassamy et al.[21] coincidentally proposed a geometric method based on the previous work of Malladi[6]. They used an arc length - based functional for the segmentation task:

$$E_{GAC}(C) = \int_0^1 g(\nabla(G * I(x, y)))|C_s(s)|ds \tag{4}$$

where $g(.)$ is a gradient-based function to extract edges on the image (similar to the functions described for the last method), C_s is the derivation of the contour C with respect to s and $|C_s(s)|ds$ is the arc length of the curve. Caselles[3] named its method as Geodesic Active Contour and he also demonstrated that this functional is equivalent to the energy function of Kass et al.[7] named "snakes" in other representation space. The solution for the segmentation is found by minimizing the last functional, which is addressed by using the calculus of variation and the gradient descent method. Therefore, the differential equation obtained from the minimization process of the functional is written as:

$$\frac{\partial C}{\partial t} = g\left(\nabla\big(G * I(x, y)\big)\right)k\boldsymbol{n} - (\nabla g \cdot \boldsymbol{n})\boldsymbol{n} \tag{5}$$

Taking into account the problems arisen from using the explicit representation of the contour, the last equation is then expressed by employing a level set formulation:

$$\frac{\partial \varphi}{\partial t} = \left[g\left(\nabla\big(G * I(x, y)\big)\right)(k + c) - (\nabla g \cdot \nabla\varphi)\right]|\nabla\varphi| \tag{6}$$

As introduced in the Malladi's method, in this case an artificial constant c is employed in the evolution equation as well. Even though this approach is similar to the last one due to the fact that it uses a gradient function in the first term of the velocity field, here we can find a second term that substantially improves the edge detection process. For this reason, the application of the geometric active contour on real images must present a better performance compared with the Malladi's[6] approach. We refer the readers to the original paper[3] for more details about the method.

2.3 Chan-Vese Functional - CVF

One of the main disadvantages of the reviewed approaches in last section is related to the use of an image characterizing function based on the image gradient, i.e., an edge detector function. It is well known that a gradient-based function generally presents poor performance in presence of noise. Moreover, the low contrast and the lack of homogeneities of real images contribute to increase the poor performance. These problems are better reflected when working with medical images.

Chan and Vese[4] intelligently created a procedure based on a level set formulation to attack the segmentation problem without using edges detector or gradient functions. It minimize substantially the errors derived from using boundary-based detection methods. The Chan-Vese method is an adaptation of the Munford-Shah[22] functional for image segmentation. They proposed a functional that takes as principal image parameter the gray level information of the regions inside and outside the contour:

$$E_{ChanVese} = \gamma_1 \int_{inside\ C} (I(x,y) - \mu_1)^2 dxdy \ + \ \gamma_2 \int_{outside\ C} (I(x,y) - \mu_2)^2 dxdy + \ \alpha Length(C) \\ + \ \beta \int_{inside\ C} dxdy \tag{7}$$

where the two first integrals are considered the data terms and they measure the homogeneity of the regions fragmented by the contour (inside and outside the contour). The functional also includes one term that measures the arc length of the curve and other that calculates the area of the region inside the contour (the last integral). The area term is put to zero for most of the applications. In the functional $\gamma_1, \gamma_2, \alpha$ and β are constants that weight each term. A level set representation of this functional was formulated as well:

$$E_{ChanVese} = \gamma_1 \int_{\Omega} (I - \mu_1)^2 H(\varphi) dxdy \ + \ \gamma_2 \int_{\Omega} (I - \mu_2)^2 (1 - H(\varphi)) dxdy + \ \alpha \int_{\Omega} \delta(\varphi) |\nabla\varphi| \, dxdy \\ + \ \beta \int_{\Omega} H(\varphi) dxdy \tag{8}$$

where $\mu_1$and μ_2 are computed as the average of the gray level data of the image by using the pixels inside and outside of the contour respectively; $H(\varphi)$ is a Heaviside function and $\delta(\varphi)$ is the Delta Dirac. As in the geometric active contour, a solution of the last functional is obtained through a minimization process (respect to φ) by using the calculus of variations and the gradient descent method, maintaining $\mu_1$and μ_2 fixed. It leads to the following partial differential equation:

$$\frac{\partial\varphi}{\partial t} = \delta(\varphi)[\alpha k - \beta - \gamma_1 (I - \mu_1)^2 + \gamma_2 (I - \mu_2)^2] = 0 \tag{9}$$

with $\varphi(o, x, y) = 0$ being the initial level set function and the condition $\frac{\delta(\varphi)}{|\nabla\varphi|} \frac{\partial\varphi}{\partial \boldsymbol{n}} = 0$. The final solution comes from resolving the partial differential equation. In[23] is stated that a sign distance function can be used instead of a Delta Dirac function in the last equation. Details about the procedure to reach the solution is out of the scope of this paper**.**

2.4 Geodesic Active Regions - GAR

This is the last method we review in our analysis. Nikos Paragios[5] developed an approach based on level set that have been extensively used for segmentation as well. Similarly, the formulation of the method for segmentation applications consists of a functional that is minimized in the desired solution. Here, a weighted combination of two terms is proposed to handle the image partition task: a region-based term and a boundary-based term. This method can be considered as a combination of the last two ones. In spite of using a region term based on an average of the gray level information of the image, Paragios[5] opted for incorporating a Bayesian estimation through a MAP (maximum a posteriori) algorithm. This implies that the method requires the computation of a probability distribution function for each image partition. Therefore, for two partitions the functional was formulated as:

$$E_{GAR}(C) = \sum_{X \,\epsilon\, (A,B)} (1 - \alpha) \int_0^1 g\left(\mathrm{p}_{\mathrm{C,X}}\big(I(C(s))\big)\right) |C_s(s)| ds - \sum_{X \,\epsilon\, (A,B)} \alpha \iint_{\Omega_{\mathrm{X}}} \log\left[\mathrm{p}_{\Omega,\mathrm{X}}(I(x,y))\right] dxdy \tag{10}$$

where the first term represents the boundary parameter, being $\mathrm{p}_{\mathrm{C,X}}\big(I(C(s))\big)$ the boundary probability and $g(\cdot)$ the boundary attraction function, and the second term is the region parameter with $\mathrm{p}_{\Omega,\mathrm{X}}(I(x,y))$ being the probability distribution. Likewise, (A, B) are the image partitions corresponding to the regions inside and outside the contour C respectively; $0 \leq \alpha \leq 1$.

As mentioned in the last methods, finding a solution implies to use the calculus of variations and the gradient descent method to minimize the objective function. Then, the following partial differential equation is obtained for the first one partition (A):

$$\frac{\partial\varphi}{\partial t} = \left[\alpha \log\left(\frac{\mathrm{p}_{\Omega,\mathrm{B}}(I(x,y))}{\mathrm{p}_{\Omega,\mathrm{A}}(I(x,y))}\right) + (1 - \alpha)\left(g\left(\mathrm{p}_{\mathrm{C,A}}\big(I(C)\big)\right) k - (\nabla g \cdot \nabla\varphi)\right)\right] |\nabla\varphi| \tag{11}$$

where a level set formulation was also used. A similar partial differential equation can be obtained for the second partition (A). As can be seen in the equation, a geodesic active contour can be used for the boundary term. Obviously, it is necessary to formulate a probability distribution for the region term. The rest of details about the method is well explained at[5].

3. MATERIALS AND IMPLEMENTATION DETAILS

3.1 Materials

In our evaluation, we have used several cardiac CT images taken from seven studies of tomography with different characteristics of contrast and resolution. Each study comes from a different patient as well, which implies that we have images with significant variations regarding the object of interest. The structure of analysis was the left ventricle using the original axial view of the tomography. The images taken for the evaluation show the left ventricle at the mid part of the heart. We address our analysis without taking care about the phase of the cardiac cycle in which the data was selected. Tomographic studies were acquired with a 16-slice CT system of SIEMENS at 120 kVp of tube voltage and 900 mA. The size of each image of the tomography is 512 x 512 pixels, quantized to 12 bits per pixel. Contrast agent were also applied on each patient.

In order to address the manual segmentation to validate the methods, we have created an interactive Matlab® graphic interface that enables the experts to mark the contour of the left ventricle in the images. The application makes possible to select specific image sequences from the cardiac CT studies to go through with the annotation process.

3.2 Some details about the algorithmic implementation

We have implemented all the methods using the Matlab® 7.13 Programming Language installed on a PC with CPU of 2.4GHz and RAM of 6 GB. For the most time-consuming processes, we used C implementation based on Mexfiles libraries, compiled with Visual Studio C++ 2010 Express. In this section, we also mention some of the most important details that we take into account to carry out the implementation of the level set algorithms. For this matter, we have employed the fast marching methods described in[24]. Since each of the analyzed approach uses particular image parameters to configure the level set evolution, we have to realize some adaptations depending on the sample images. These adaptations become an essential task because of the level set approaches are set up to stop the propagation at the object boundaries. We summarize the implementation details as follows.

1) The boundary-based methods (Shape extraction method of Malladi et al.[6] and Geodesic Active Contour[3]) are designed to stop the evolution of the level set function at positions where the gradient of the images is relatively high. For real images, as the cardiac CT examples used here, the gradient that defines the edge of the analyzed object changes significantly from one example to other. With the simple gradient-based monotonically decreasing function described in section 2.1 and 2.2, the evolution process does not work efficiently for each example. This is due to the varying contrast, noise and poor definition of edges. In this part, we used a step function to threshold the gradient-based function at the boundaries of the objects:

$$step(V) = \begin{cases} V(x,y) & if \quad V(x,y) \leq T \\ 0 & if \quad V(x,y) > T \end{cases} \tag{12}$$

where the threshold T is experimentally and manually selected from the image histogram; $V(x,y)$ is the field velocity of the level set at the position (x,y).

2) The region-based approaches are more suitable to handle the problems related to the variations of the input images. For the *Chan-Vese Functional* we average the gray level of the regions inside and outside the active contour to compute the parameters μ_1 and μ_2 respectively. This computation is made in each iteration. For the *Geodesic Active Region* method, we assume Gaussian probability distribution for the regions. Standard deviation and mean of the Gaussian function were experimentally obtained from the input image. As in the CVF method, the Gaussian parameters in the GAR approach can be computed in each iteration. Instead, we calculate them one time by selecting two windows from the image: the first window is taken inside the region of the left ventricle and the second one is obtained in the region of the septum. Thereby, we could reduce the computation time of the GAR method.

3)It has been demonstrated that the distance function in methods based on level set must be re-initialized to avoid degradations that can lead to errors in the evolution process[18-19]. The period to re-initialize the level set function in this work was experimentally chosen for each example.

4)Finally, since the field velocity in all the methods includes diverse types of terms (contour-based terms and image-based terms), we have to normalize them to the same range of variation to avoid bias in the results caused by any of them.

4. RESULTS AND DISCUSSIONS

As mentioned, the methods are evaluated in seven images taken from cardiac CT studies. Each method is applied on both the original images and the filtered version of them. We use common Gaussian filters for smoothing the images. In this section, we address quantitative and qualitative analysis of the approaches. We also make subjective comparison among the obtained findings. Even though the initialization for segmentation tasks using approaches based on level sets is not a critical requirement, we try to use the same initial contour to maintain a standard experiment. This initialization was manually put on the images. We selected a point in the images to drawn the initial contour around it, which consist of a circular shape with a radius *r*. Regarding the boundary-based methods, in this section we only show results of the Geodesic Active Contour approach.

In figure 1 we observe three of the seven sample images that we used for the evaluation. As shown, there are significant differences related to the image contrast and shape of the left ventricle. Additionally, the initial contour, manually put on the images, is visualized.

The best obtained results of the each method applied on the images shown in figure 1 are illustrated in figures 2 and 3. As can be seen, the Geodesic Active Contour method does not present acceptable visual result; "leaking" problems of the level set function are notable in the boundary of the object. Figure 4 illustrates other visual results for other image of our dataset.

In the quantitative analysis, we use a point-to-curve distance metric to estimate the approximated error of the segmentation. The comparison is made against the manual segmentation, which is obviously made by the expert. Here, we address the comparison between the two region-based methods because in the Geodesic Active Contour was not possible to achieve a stable solution for all the examples. The reason was the "leaking" problems of the level set function out of the boundary of the objects. In table 1, we depict the obtained results which are put in pixel values. These results corresponds to the average Euclidean distance per point.

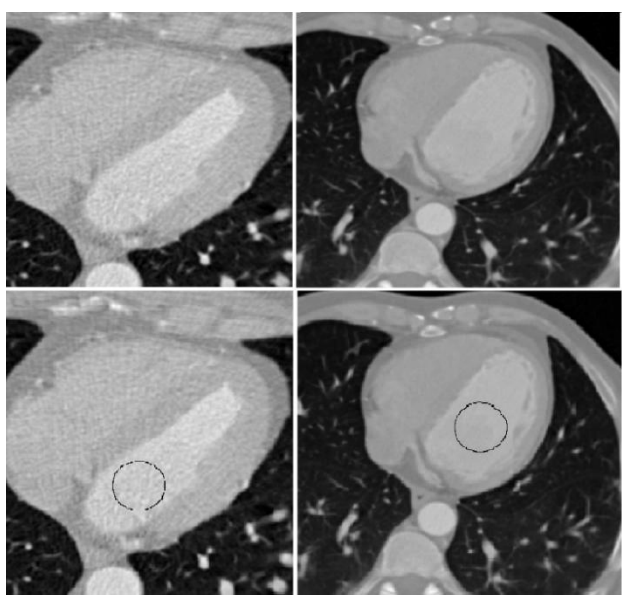

Figure 1. Sample images and the initial circular contours used for each of them.

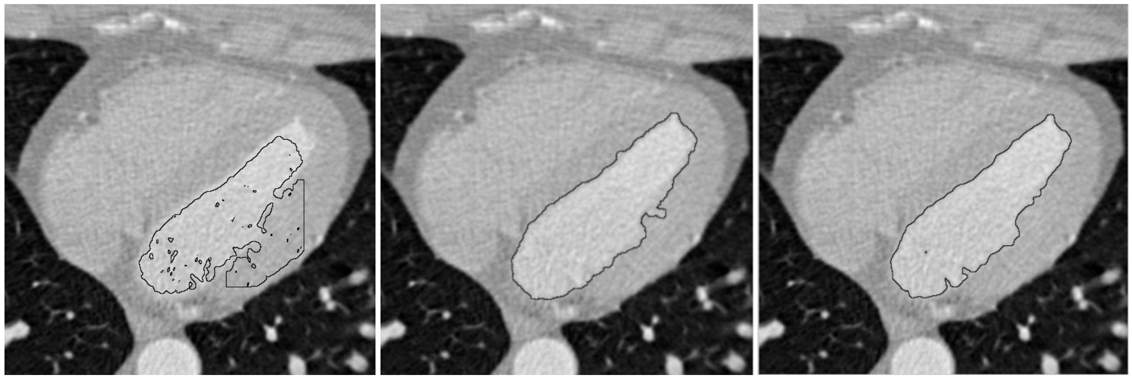

a) b) c)

Figure 2. Segmentation results by using the first image of figure 1with the method: a) Geodesic Active Contour, b) Chan-Vese Functional and c) Geodesic Active Region.

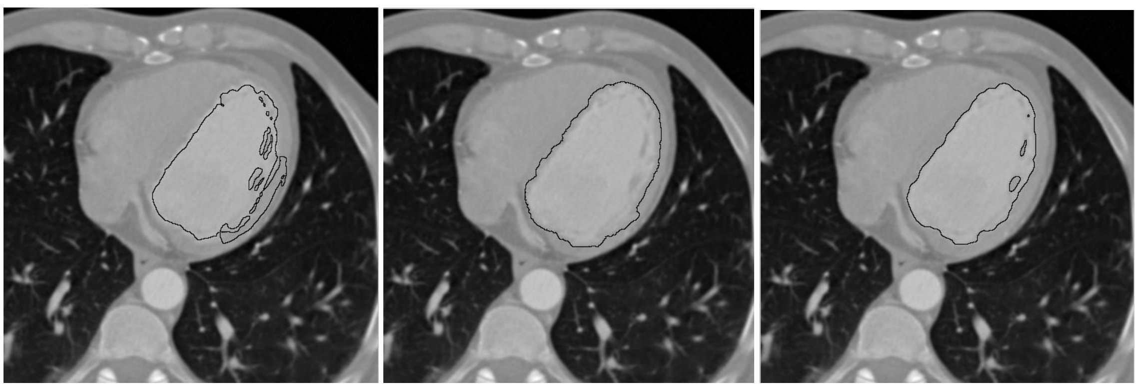

a) b) c)

Figure 3. Segmentation results by using the second image of figure 1with the method: a) Geodesic Active Contour, b) Chan-Vese Functional and c) Geodesic Active Region.

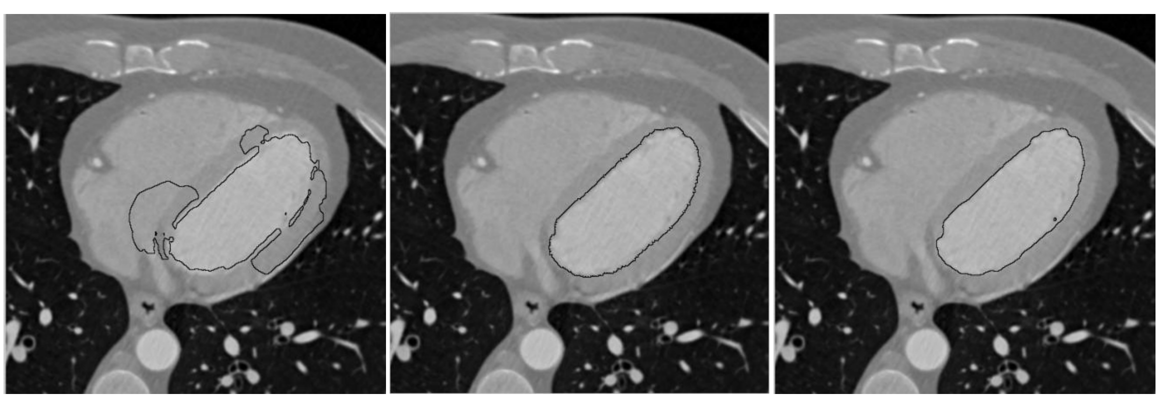

a) b) c)

Figure 4. Segmentation results by using other image example with the method: a) Geodesic Active Contour, b) Chan-Vese Functional and c) Geodesic Active Region.

Table 1. Point-to-Curve Distance measure for results obtained with the CVF and GAR methods.

Test Images	CVF Method (mean ± std)	GAR Method (mean ± std)
Image 1	4.1324 ± 4.0704	3.2721 ± 4.3418
Image 2	1.8666 ± 1.3579	2.5183 ± 3.1299
Image 3	3.8008 ± 2.3404	2.3120 ± 2.3305
Image 4	7.1218 ± 3.8059	4.8308 ± 4.0378
Image 5	6.7199 ±3.7648	4.0989 ± 2.8884
Image 6	3.7145 ± 2.9439	3.8066 ± 2.9900
Image 7	5.7558 ± 4.4906	5.6664 ± 4.9738

Some details as the re-initialization period, selection of the parameters values for each method and the types of filters to apply in each example were defined from the experiments. The weight parameter α for the GAR method, the constants α, β, γ_1 and γ_2 of the CVF method and the threshold T in the GAC method are part of this experimental selection. We have made a preliminary analysis of the gray level information of the images in order to choose the parameter values. Even though special effort has been made by many authors to automatically solve these problems, it is still a very hard and difficult task. A better result was obtained giving a bigger weight to the region term in the GAR method. In table 2, we also present sensitivity and specificity measures to quantify the binary detection of the regions of interest for each example by using the CVF and GAR methods.

Table 2. Sensitivity and specificity measures for results obtained with the CVF and GAR methods.

Test Images	Sensitivity		Specificity	
	CVF Method	GAR Method	CVF Method	GAR Method
Image 1	0.9574	0.9286	0.9874	0.9907
Image 2	0.9913	0.9725	0.9965	0.9989
Image 3	1.0000	0.9720	0.9910	0.9979
Image 4	0.9999	0.9781	0.9852	0.9959
Image 5	0.9967	0.9394	0.9825	0.9968
Image 6	0.9985	0.9659	0.9896	0.9976
Image 7	0.8789	0.8910	0.9992	0.9990

4.1 Discussions

From the visual results, we can infer that the best performance is obtained with the region-based methods (CVF and GAR). Although the approximation is good in both cases, there are two marked differences to analyze here from our implementation. These differences can be very useful at the moment to chose a method. 1) The GAR method is more sensible to the gray level variation than the CVF approach. For these examples, it was reflected in such a way that regions of the papillary muscle were segmented in the left ventricle when using GAR. Parts with small gray variations are extracted as well. This behavior is not attractive in applications for segmenting the left ventricle. 2) On the other hand, the CVF method is slower than the GAR approach. In applications where the amount of data is critical, having faster algorithms is more convenient. Although CVF method can be considered as a particular case of the GAR approach when using Gaussian distribution in the region term, the GAR method also includes a boundary term to assist in the segmentation task. It represents a significant increment of the computation time. With the same period of re-initialization, in our implementation we obtained differences close to 100 iterations between the convergences of both methods. From table 1, we can see that the results achieved are very similar. There are not remarkable differences about the quantitative analysis between the methods (CVF and GAR). Errors as the segmentation of the papillary muscle are not visible with the distance metric. These errors are found with the GAR and GAC methods (see figure 3a and 3c). The main reason is the boundary term which is included in both methods. However, table 1 shows acceptable approximation for the segmentation achieved in both methods. Results specified in table 2 show that a better detection rate for the left ventricle was achieved with the CVF method (sensitivity) while a best specificity for all cases was obtained with the GAR method. Table 2 reflect very short differences between the performances of both methods as well.

The gray level information in the CVF method represents the most significant contributor for the segmentation task. This could indicate that others regions of the images that have similar gray values to the left ventricle should be segmented as well. However, in our implementation we used signed distance functions as the level set function. As indicated in last figures, these objects are far-off the left ventricle, and even more far-off the initial contour. It implies that bigger distance values are assigned in those regions, avoiding the segmentation of those objects. Moreover, the re-initialization process contributes to prevent the segmentation of those undesired regions.

The GAC method fails to segment all the left ventricle of the images in figures 2 and 3. The reason is that the edge detection process by using the functions described in the last section does not work perfectly in the object boundary. Poor definitions of edges and low contrast cause this behavior, i.e. the complete boundary of the object is not characterized with similar gradient magnitudes. This behavior is spread out in all the examples.

5. CONCLUSION

We have developed a comparative study of the most popular segmentation methods based on level sets for shape extraction in cardiac CT images. The methods were implemented and compared by using qualitative and quantitative analysis. The region-based approaches (GAR and CVF) presents enormously better results than the boundary-based methods for the cardiac CT images. Better edge detection functions are needed in these types of segmentations. In all cases, the best result was obtained with the filtered version of the input images. Finally, for these application's types is completely necessary to introduce prior information to the formulation of the methods. Geometrical knowledge, gray level distributions and texture are common prior information used to handle the segmentation problem. The work can be serve as a base to chose a method for this and others applications.

ACKNOWLEDGEMENT

This work was supported by UNAM grant PAPIIT IN113611 and UNAM-CEP. Authors thanks reviewers for their valuable comments about the paper.

REFERENCES

[1] Bagci, U., Udupa, J. K., Mendhiratta, N., Foster, B., Xu, X., Yao, J., Chen, X. and Mollura, D. J., "Joint segmentation of anatomical and functional images: applications in quantification of lesions from PET, PET-CT, MRI-PET, and Mri-PET-CT images," Medical Image Analysis 17(8), 929-945 (2013).

[2] Niessen W., [Model-Based Image Segmentation for Image-Guided Interventions, Image-Guided Interventions - Technology and Applications], Springer-Verlag Publisher, Berlin Heidelberg, 219-239 (2008).

[3] Caselles, V., Kimmel, R. and Sapiro, G., "Geodesic active contours," Proc. Int. J. Comput. Vis. 22(1), 61–79 (1997).

[4] Chan, T. and Vese, L., "Active contours without edges," IEEE Trans. Image. Process. 10(2), 266–277(2001).

[5] Paragios, N. and Deriche, R., "Geodesic active regions: a new paradigm to deal with frame partition problems in computer vision," Journal of Visual Communication and Image Representation 13, 249–268 (2002).

[6] Malladi, R., Sethian, J. A. and Vemuri, B. C., "Shape modeling with front propagation: A level set approach," IEEE Trans. Pattern Anal. Mach. Intell. 17(2), 158–175 (1995).

[7] Kass, M., Witkin, A. and Terzopoulos, D., "Snakes: Active contour models," Int. J. Comp. Vision 1, 321–331 (1988).

[8] Cootes, T.F., Taylor, C.J., Cooper, D.H. and Graham, J., "Active shape models - their training and application," Computer Vision and Image Understanding 61(1), 38–59 (1995).

[9] Cootes, T. F., Edwards, G. J. and Taylor, C. J., “Active appearance models,” Proc. European Conference on Computer Vision 2, 484-498 (1998).
[10] Osher, S. and Sethian, J. A., "Fronts propagating with curvature-dependent speed: Algorithms based on Hamilton-Jacobi formulations." Journal of Computational Physics 79(1), 12–49 (1988).
[11] Kadir, K., Gao, H., Payne, A., Soraghan, J. and Berry, C., "LV wall segmentation using the variational level set method (LSM) with additional shape constraint for oedema quantification," Phys. Med. Biol. 57 (19), 6007-23 (2012).
[12] Woo, J., Byung-Woo, H., Ramesh, A., Germano, G., Jay Kuo, C.-C. and Slomka, P., "Curve evolution with a dual shape similarity and its application to segmentation of left ventricle," Proc. SPIE 7259, (2009).
[13] Osher, S. and Paragios, N., [Geometric Level Set Methods in Imaging, Vision and Graphics], Springer Publisher, New York, 1-513 (2003).
[14] Yan, J. Y. and Zhuang, T., “Applying improved fast marching method to endocardial boundary detection in echocardiographic images,” Pattern Recognit. Lett. 24(15), 2777–2784 (2003).
[15] Woo, J., Slomka P. J., Jay Kuo, C.-C. and Byung-Woo H., "Multiphase segmentation using an implicit dual shape prior: Application to detection of left ventricle in cardiac MRI," Computer Vision and Image Understanding 117 (9), 1084-1094 (2013).
[16] Dedic, R., Madjid, A. and Lecomte, R., "Unsupervised cardiac PET image segmentation," Proc. Conference on Systems, Signals and Image Processing (IWSSIP), 1-6 (2011).
[17] Chao, L., Xiao, J. and Ying, S., "Improved semi-automated segmentation of cardiac CT and MR images," Proc. IEEE International Symposium on Biomedical Imaging: From Nano to Macro, 25-28 (2009).
[18] Chunming, L., Chenyang, X., Changfeng, G. and Fox, M.D., “Level set evolution without re-initialization: a new variational formulation,” Proc. IEEE Conference on Computer Vision and Pattern Recognition, 430-436 (2005).
[19] Estellers, V., Zosso, D., Lai, R., Osher, S., Jean-Philippe T. and Xavier Bresson, "Efficient Algorithm for Level Set Method Preserving Distance Function," IEEE Transactions on Image Processing 21(12), 4722-4734 (2012).
[20] Mitiche, A. and Ben Ayed, I., [Variational and Level Set Methods in Image Segmentation], Springer-Verlag Publisher, Berlin Heidelberg, 15-57 (2010).
[21] Kichenassamy, S., Kumar, A., Olver, P., Tannenbaum, A. and Yezzi, A., “Gradient flows and geometric active contour models,” Proc. 5th Int. Conf. Comput. Vis., 810–815 (1995),
[22] Mumford, D. and Shah, J., “Optimal approximations by piecewise smooth functions and associated variational problems,” Commun. Pure Appl. Math. 42(5), 577–685 (1989).
[23] Osher, S. and Fedkiw, R., [Level set methods and dynamic implicit surfaces], Springer Publisher, New York, 1-124 (2003).
[24] Sethian, J. A., [Level Set Methods and Fast Marching Methods], Cambridge University Press, Cambridge, (1999).